Universal form of the power spectrum of the aero-optical aberration caused by the supersonic turbulent boundary layer*

Gao Qiong(高 穹)[a)†], Yi Shi-He(易仕和)[b)], and Jiang Zong-Fu(姜宗福)[a)]

[a)] College of Photon–Electron Science and Engineering, National University of Defense Technology, Changsha 410073, China
[b)] College of Aerospace Science and Engineering, National University of Defense Technology, Changsha 410073, China

(Received 5 December 2013; revised manuscript received 10 February 2014; published online 10 August 2014)

Based on the measurement of one-dimensional (1D) optical path difference (OPD) of the supersonic turbulent boundary layer, an analytical form for the power spectrum of the two-dimensional (2D) OPD is obtained with its structure function and under the locally homogeneous isotropic assumption. The universality of this spectrum is argued, and its validity is checked by the comparison with experimental result. The potential applications of this model in theoretical and numerical studies are emphasized. Another contribution of this work is around the application of correlation function to analyzing the statistics of OPD. Based on our results and other results published elsewhere, we show that the OPD is often not stationary, and one should be cautious about using this tool.

Keywords: aero-optics, supersonic turbulent boundary layer, optical path difference, power spectrum

PACS: 42.25.Dd, 47.40.Ki **DOI:** 10.1088/1674-1056/23/10/104201

1. Introduction

The aero-optical aberration caused by the compressibility of high speed flow field is an important problem for developing airborne optical systems, especially for the supersonic and hypersonic vehicles, and has attracted much attention for many decades.[1–4] In most applications the optical path difference (OPD) is often used to characterize the aberration. The turbulent boundary layer (TBL) is one of the most important building block flows for the study of aero-optics, and understanding the structure of its OPD is critical for characterizing the optical imaging or beam propagating through the flow. Gordeyev *et al.*[5] performed the extensive experimental study of optical aberrations due to propagation through subsonic turbulent boundary layers (SBTBL) by using the small aperture beam technique (SABT).[6] Their results indicated that the optical distortion was found to scale linearly with boundary layer thickness and freestream density, and to go as the square of the free stream Mach number. Using a similar experimental technique, Wittich *et al.*[7] analyzed the spanwise and streamwise correlation functions of the jitter signal caused by the SBTBL, and proposed a method of simulating the wavefront by constructing a model for its power spectrum. Smith *et al.*[8] reported the aero-optical distortions of the SBTBL using a high-speed Shack–Hartmann sensor, and analyzed the aberrated wavefront from the viewpoint of power spectrum. Wang K and Wang M[9] carried out the large eddy simulation to study the aero-optical distortions of the SBTBL. The effects of aperture size, small-scale turbulence, different flow regions, and beam elevation angle were examined and the underlying flow physics was analyzed. Wyckham and Smits[10] measured the aero-optical distortion due to the transonic and hypersonic TBL with Shack–Hartmann sensor, and proposed a scaling law for the root-mean-square of phase distortion, which can collapse the data under different experimental conditions quite well. Gordeyev *et al.*[11] performed the aero-optical measurements of a supersonic turbulent boundary layer (SPTBL) with Malley probe, and found a new scaling law which is consistent with the law of Wyckham *et al.* over a wide range of Mach numbers.

One may note that the experimental researches mentioned above used either the SABT or the Shack–Hartmann sensor. What the SABT measures are the temporal jitter signals at a few locations, and the assumption of frozen hypothesis needs to be made to obtain the spatial distribution of the optical distortion. The recent progress of Shack–Hartmann sensor makes it available to respond to the temporal variation of aero-optical distortion, but its spatial resolution is not sufficient to resolve the structure of the distortion in many important cases. Being different from these studies, this work is based on the measurement of flow density with high spatial-temporal resolutions. Using the structure function of OPD obtained experimentally and under the locally homogeneous isotropic assumption, a universal form for the power spectrum of the 2D OPD is proposed.

*Project supported by the National Natural Science Foundation of China (Grant No. 61008037) and the National Basic Research Program of China (Grant No. 2009CB724100).

†Corresponding author. E-mail: gaoqiong1980@126.com. Present address: Key Laboratory of Electro–Optical Countermeasures Test & Evaluation Technology, Luoyang 471003, China.

© 2014 Chinese Physical Society and IOP Publishing Ltd

2. Experiment

The experimental setup used in this study consists mainly of the supersonic wind tunnel with Mach number $M_\infty = 3.0$ and the nanoparticle-based planar laser scattering (NPLS) system. The wind tunnel is direct-linked in structure, and the nozzle is designed by the method of B-spline function. The size of the test section is 100 mm×120 mm, and the measurements are made on the SPTBL developed on the wall of the test section. Some important parameters of the SPTBL are listed in Table 1. The NPLS system uses the TiO_2 particles of nominal size 18 nm as tracers, which are mixed into the air at the entrance of the wind tunnel. A thin pulsed laser sheet (double-cavity laser, wavelength: 532 nm, pulse width: 6 ns, energy per pulse: 400 mJ, thickness of the sheet: 0.5 mm) is used to illuminate the flow region of interest. The light scattered by the nanoparticles is received by an interline transfer charge coupled device (CCD). The time interval between two exposures is controlled by synchronizing the laser and CCD, and the smallest interval can reach 0.2 μs. More details about NPLS and its application in visualizing the boundary layer can be found in Refs. [12]–[15]. Tian *et al.*[16] have suggested a calibration procedure to convert the pixel value of NPLS image into dimensional density. The basic idea is to place a wedge with adjustable attack angle, and obtain calibration parameters by using the density relation before and behind the shock wave.

Table 1. Important flow parameters of the SPTBL with $M_\infty = 3.0$.

ρ_∞/kg·m^{-3}	P_0/kPa	T_0/K	δ/mm	λ_B/μm	C_f
0.0912	101	294	10.2	5	1.7×10^{-3}

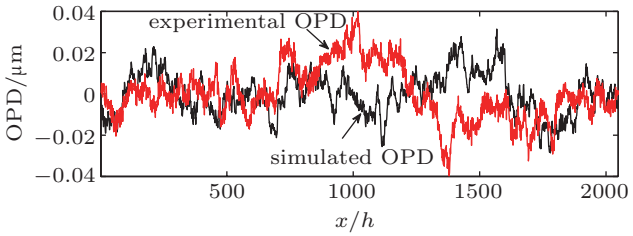


Fig. 1. (color online) OPD of the SPTBL obtained from the experiment and numerical simulation.

We obtain 200 OPDs in the experiment, and figure 1 shows such an example with the line indicated by 'experimental OPD'. Because the light source in the NPLS system is a pulsed laser with pulse width 6 ns, the measurement can be regarded as being instantaneous. The physical size relevant to the OPD is 27 mm along streamwise direction, and the length of the signal is 2048 so the digital resolution is $h = 0.013$ mm. Before further analysis, we check our experimental results by computing the root mean square of OPD (OPD_{rms}), and compare it with theoretical predictions. Here we use the scaling model of OPD_{rms} suggested by Wyckham and Smits,[10] which can be written as

$$\Delta \equiv \mathrm{OPD}_{\mathrm{rms}}/(C_w K_{GD}\rho_\infty \delta M_\infty^2 \sqrt{C_f}) = r_2^{-3/2}. \quad (1)$$

Here, K_{GD} is the Gladstone–Dale constant, ρ_∞ is the density of free stream, δ is the thickness of the SPTBL, and C_f is the skin friction coefficient. The model parameter C_w is often set to be 0.34, and

$$r_2 = 1 + M_\infty^2(\gamma-1)(1-rr_c^2)/2, \quad r_c = U_c/U_\infty \quad (2)$$

for the adiabatic wall, where $\gamma = 1.4$ is the heat capacity ratio, $r = 0.9$ is the recovery factor, and U_c is the convection velocity of the large scale optical structure. When using this scaling law, the term Δ on the left-hand side in Eq. (1) is computed with the experimental parameters, and compared with the theoretical prediction on the right-hand side. With the experimental parameters, we obtain $\Delta = 0.150$. With the result of Gordeyev *et al.*,[11] the values of r_c are 0.82 for subsonic boundary layer and 0.84 for supersonic case respectively. The values of the term on the right-hand side of Eq. (3) are 0.152 with $r_c = 0.82$, and 0.159 with $r_c = 0.84$ respectively. So our experimental result is in agreement with that from the theoretical model.

3. Power spectrum of OPD

For stationary random field, we know that the power spectrum is the Fourier transform of correlation function, so the correlation function can be taken as a starting point for analysis. Usually, the correlation coefficient of OPD can be computed with

$$\mu(x) = \langle \mathrm{OPD}(x+x_0)\mathrm{OPD}(x_0)\rangle / \langle \mathrm{OPD}^2(x_0)\rangle, \quad (3)$$

where the angle brackets denote the average over x_0 and the ensemble. The results are shown in Fig. 2 with open circles, and the results of Gordeyev *et al.*[11] obtained by SABT are also given with open triangles in this figure for comparison. In contrast to the results of subsonic boundary layer, the correlation coefficient of the SPTBL has a negative local minimum, indicating weak periodic structures in the streamwise direction.

By examining the correlation coefficients carefully, we find that the following empirical model can fit the data quite well:

$$\mu(x) = \mathrm{e}^{-x/\gamma}(1 + a_1 x + a_2 x^2 + a_3 x^3), \quad x \geq 0, \quad (4)$$

where the parameter γ can be regarded as the characteristic length and the polynomial in the parenthesis modulates the exponential function for large x. Using the data for the $M_\infty = 3.0$ flow and the data for the $M_\infty = 3.0$ flow, the nonlinear least-square gives

$$\gamma = 0.2837, \quad a_1 = -4.9375, \quad a_2 = 12.2506, \quad a_3 = -14.4191,$$

and the model parameters for the $M_\infty = 2.0$ flow are

$$\gamma = 0.5269, \quad a_1 = -0.5930, \quad a_2 = -2.4907, \quad a_3 = -0.0010.$$

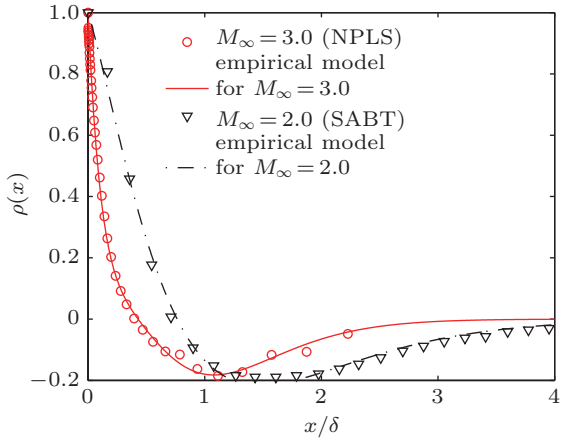


Fig. 2. (color online) Correlation coefficients of the OPD and the fitted curves with the empirical model in Eq. (4).

The two fitting curves using the sets of parameters are displayed in Fig. 2, and the fitting performance is remarkable. Imagine a 2D isotropic OPD with correlation function of the form in Eq. (4), its 2D power spectrum of OPD can be expressed by the Hankel transform

$$\Phi(k) \propto \int_0^\infty r\mu(r) \mathrm{J}_0(2\pi kr)\,\mathrm{d}r, \tag{5}$$

where J_0 is the Bessel function of zero order, and r and k are the amplitudes of 2D space vector and frequency respectively. Substituting Eq. (4) into Eq. (5), we can obtain[17]

$$\Phi(k) \propto \sum_{\nu=1}^{4} a_{\nu-1} \frac{2^\nu \Gamma\left(\frac{\nu+1}{2}\right)\Gamma\left(1+\frac{\nu}{2}\right)}{(k^2+k_0^2)^{\nu+1/2}} \times {}_2\mathrm{F}_1\left(\frac{\nu+1}{2}, -\frac{\nu}{2}; 1; \frac{k^2}{k^2+k_0^2}\right), \tag{6}$$

where ${}_2\mathrm{F}_1\,(a, b; c; z)$ is the hypergeometric function, $k_0 = 1/\gamma$ is the characteristic frequency and we assume $a_0 = 1$. With the fitted parameters, the terms on the right-hand side of Eq. (6) can be computed numerically, and the results are shown in Fig. 3. A surprising feature of Fig. 3 is that the spectrum is negative at small frequency, contradicting the non-negative requirement of the power spectrum of a stationary random field. So the OPD of the two flows concerned here cannot be regarded as being stationary, and there is no sufficient argument for defining the correlation function. This phenomenon can be accounted for by the hairpin vortices packets meandering for very long streamwise distance,[18–20] which makes the OPD non-stationary along the streamwise direction.

In order to relax the requirement for the statistics of OPD, we resort to the tool of structure function, which assumes the stationary increment and is used frequently in analyzing the signal related to turbulence. With the ensemble of OPD obtained in our experiment, we compute its structure function as

$$D(x) = \langle (\mathrm{OPD}(x+x_0) - \mathrm{OPD}(x_0))^2 \rangle. \tag{7}$$

The results are shown in Fig. 4 by open circles in double logarithmic coordinate, from which we can find the distinct power law behavior over a wide range of distance. Using the equation of the fitted line in Fig. 4, the structure function can be written as

$$D(x) = D_0^2 x^\mu, \quad \mu = 0.72, \tag{8}$$

where D_0 is a constant for the structure function.

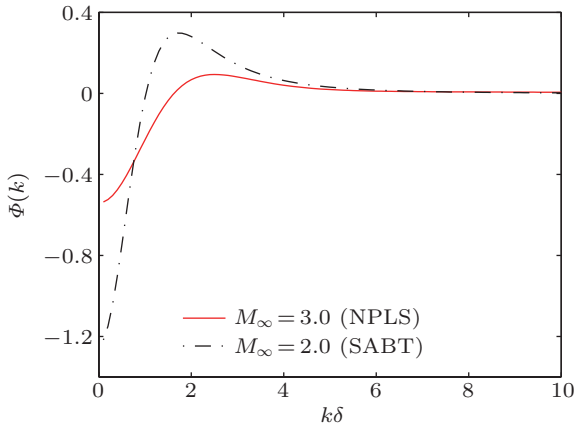


Fig. 3. (color online) Power spectrum of the two SPTBLs computed with the correlation coefficient model in Eq. (4). The unimportant constant has been omitted.

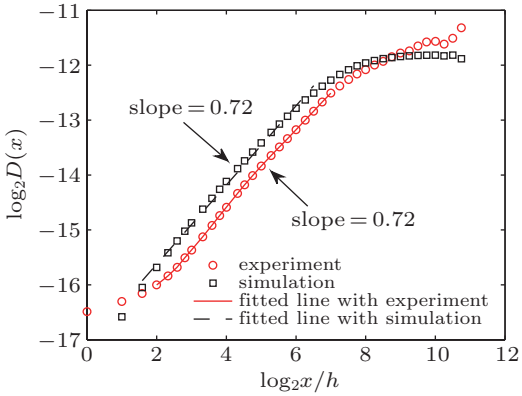


Fig. 4. (color online) Structure functions of the OPD.

Based on our visualization of the SPTBL in spanwise plane with NPLS technique, no obvious directional feature is found.[13,14] So the 2D OPD, essentially the integral of density along the vertical direction, can be considered as being locally homogeneous isotropic. Under this assumption, the power spectrum of 2D OPD $\Phi(k)$ can be expressed with the structure function as[21]

$$\Phi(k) = -\pi \int_0^\infty rD(r)\mathrm{J}_0(2\pi kr)\,\mathrm{d}r. \tag{9}$$

Assuming that the relation in Eq. (8) is valid for $x = 0$ to ∞ temporally, and substituting it into Eq. (9), we obtain

$$\Phi(k) = C_0^2 k^{-(2+\mu)}, \quad C_0^2 = \frac{\mu^2 D_0^2}{8\pi^{\mu+2}} \Gamma^2\left(\frac{\mu}{2}\right) \sin\left(\frac{\pi\mu}{2}\right), \quad (10)$$

where $\Gamma(x)$ is the Gamma function. In order to make the spectrum more analytic, we follow the treatment in the atmospheric optics[22] and modify Eq. (10) as

$$\Phi(k) = \frac{C_0^2 \exp(-k^2/k_M^2)}{(k^2 + k_m^2)^{1+\mu/2}}, \quad (11)$$

where the two characteristic frequencies k_m and k_M are defined as

$$k_m = 1/\delta, \quad k_M = 1/\lambda_B. \quad (12)$$

Here, we take the thickness δ and the Batchelor scale λ_B of the flow as the outer and inner scales. Equation (11) is the power spectrum of the 2D OPD we proposed. Comparing this expression with the phase spectrum in the atmospheric optics is useful. The parameter C_0 describes the strength of the aero-optical aberration, which plays a role similar to the Fried coherence length r_0. The thickness of a boundary layer is often used to measure the scale of coherent structure, and the Batchelor scale can be regarded as the smallest scale discussed in compressible turbulence. So the similarity between the outer and inner scales of the two spectra is obvious. The spectrum of three-dimensional (3D) phase perturbation in atmospheric turbulence obeys a $k^{-11/3}$ law. When restricted to a 2D plane, the 2D phase follows a $k^{-8/3}$ law (with a similar treatment used in Eq. (15) below). One can see that the exponents of the two spectra are in good agreement. The exponent -2.72 here is obtained from a specific experiment and may depend on the specific flow condition (the agreement between the two exponents implies that this dependence may be weak). But it is the locally homogeneous isotropic assumption that is the key in obtaining the spectrum in Eq. (11). Even if the exponent μ in a certain case is very different from the value obtained here, this assumption will still lead to a power spectrum of the form in Eq. (11). To avoid the singularity of the spectrum at zero and make the structure function approach to a constant for distance larger than a given value, modifying it into the expression in Eq. (11) is a natural and simple way. So we can regard Eq. (11) as a universal form for the power spectrum of the aero-optical aberration due to the SPTBL.

4. Validation of the power spectrum model

Now we check the spectrum model by generating 2D OPDs with it, and compare the statistics of the simulated OPD with the experimental results. Generating a random phase screen with a given spectrum is an important problem in the atmospheric optics, and many efficient algorithms have been developed to solve it. Here we adopt the common method based on FFT, and the subharmonic approach[23] is incorporated to improve the accuracy at low frequency. Choosing a proper C_0 is crucial for the simulation. Although this parameter has an analytical expression as shown in Eq. (10), a method not requiring the measurement of OPD is much more useful. Here we give an empirical method. Given the basic flow parameters, $\mathrm{OPD}_{\mathrm{rms}}$ can be computed from Eq. (1). With an initial guess of C_0, an ensemble of 1D OPD can be generated and the $\mathrm{OPD}_{\mathrm{rms}}$ can be obtained. By comparing the value with the one determined by the flow parameters, we can adjust C_0 until the $\mathrm{OPD}_{\mathrm{rms}}$ of the simulated OPD matches the desired value. Because of the linear relationship between C_0 and $\mathrm{OPD}_{\mathrm{rms}}$, a proper C_0 can be obtained after 2 or 3 rounds of simulations. With $\mathrm{OPD}_{\mathrm{rms}} = 0.011$ μm in our experiment, the matched C_0 is 1.45×10^{-4} $[\mu\mathrm{m}]^{1-\mu/2}$. In the implementation of subharmonic approach, three low-frequency screens are used, and the frequency grid spacing for each screen is $\Delta f_p = 1/(3^p L)$ with $1 \le p \le N_p$. Frehlich showed that good agreement with theory can be obtained by setting $N_p = 3$.[24] Using the flow parameters shown in Table 1, a random implementation of 2D OPD obtained in this way is shown in Fig. 5. The sampling interval is 13 μm, the digital size of the image is 2048×2048, and the dimension of the color bar is μm. Although the whole distribution is irregular, there exist many coherent optical structures of small size. A 1D slice of the 2D OPD is also given in Fig. 1 for the comparison with the experimental result. One can find that the two OPDs are almost indistinguishable by visual inspection.

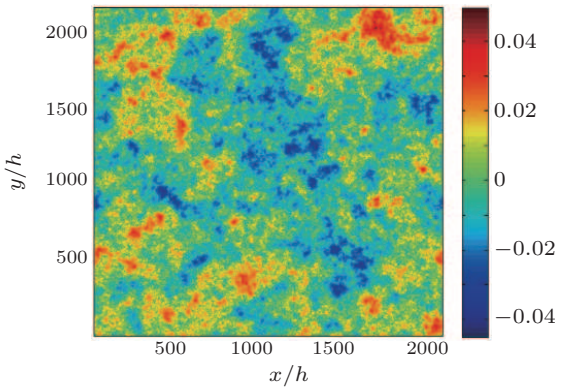


Fig. 5. (color online) Random implementation of 2D OPD.

An ensemble consisting of 1600 1D OPDs is generated by simulation, and the structure function is computed and shown in Fig. 4 with open squares. One can see that the slope of the fitted line over the intermediate region is also about 0.72. In addition, the simulated structure function approaches to a constant for large distance which is an expected property. With the relationship between $\mathrm{OPD}(x)$ and the jitter signal $\theta(t)$,[11]

the normalized amplitude spectrum of $\theta(t)$ can be written as

$$|\Theta(St_{\delta*})| = 2\pi k\phi^{1/2}(k)/\mathrm{OPD}_{\mathrm{rms}}, \tag{13}$$

where $\phi(k)$ is the power spectrum of 1D OPD, and $St_{\delta*} = f\delta^*/U_\infty$ is the Strouhal number with displacement thickness δ^*. The time frequency f and the space frequency k are related by $f = kU_c$. For $M_\infty = 3.0$, the displacement thickness can be computed to be $\delta^* = \delta/3.17 = 3.22$ mm.[25] With the ensemble of OPD, the normalized spectrum is computed and shown in Fig. 6 with solid line. This spectrum increases according to a power law for small $St_{\delta*}$ and decays slowly after a peak, which is similar to the result of Gordeyev *et al.* for $M_\infty = 2.0$.[11]

Careful examination shows that $\Theta \sim (St_{\delta^*})^\nu$ for small St_{δ^*} with $\nu = 0.13$. This relation can be examined analytically. Assuming that the spectrum in Eq. (10) is valid for all k, we can write the 1D spectrum as

$$F(k_1;y) = 2C_0^2 \int_0^{+\infty} \frac{\cos(2\pi k_2 y)\,\mathrm{d}k_2}{(k_1^2+k_2^2)^{1+\mu/2}}, \tag{14}$$

where k_1 and k_2 are the two components of a 2D space frequency. We can prove that

$$F(k_1;y) = \frac{\sqrt{\pi}C_0^2}{2^{(\mu-1)/2}\Gamma(1+\mu/2)} \times \frac{1}{k_1^{1+\mu}}(2\pi k_1 y)^{(1+\mu)/2}\mathrm{K}_{(1+\mu)/2}(2\pi k_1 y), \tag{15}$$

where K_ν is the Bessel function of the second kind with imaginary argument. Because of the complexity of this expression, it is difficult to rewrite it into a form of power law. But if assuming $k_1 y \approx 1$, we can obtain

$$F(k_1;y) \sim k_1^{-(1+\mu)} = k_1^{-2}k_1^{1-\mu}. \tag{16}$$

One can find that the exponent $(1-\mu)/2 = 0.14$ is very close to $\nu = 0.13$ obtained above.

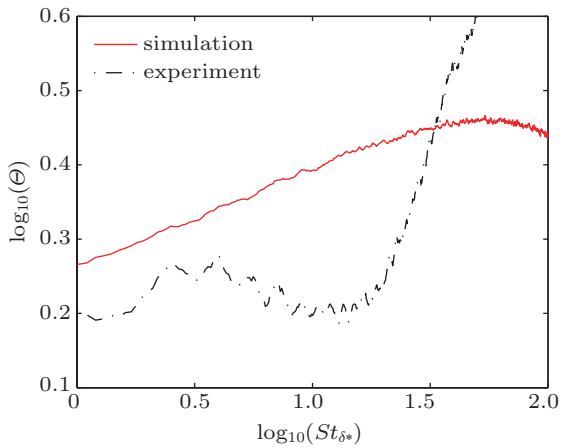


Fig. 6. (color online) Normalized amplitude spectrum of the jitter signal obtained by numerical simulation and experiment.

It is noted that the normalized spectrum of the jitter can also be computed by doing the FFT of the experimental ensemble of OPD, which is shown in Fig. 6 with the dashed line. This curve oscillates at small St_{δ^*}, and increases exponentially for large St_{δ^*}. Obviously, this result is quite different from the simulation result and other results published elsewhere.[8,11] The reason for this phenomenon may be due to the experimental noise which contaminates the computation of FFT. It seems that the method of structure function can restrain the noise effectively, and the result based on it matches others better.

5. Conclusion

In this paper, we proposed a universal form for power spectrum of the 2D OPD of the SPTBL by using the structure function and making the locally homogeneous isotropic assumption. Because of the dominant status of the OPD in aero-optics, an analytic expression of its spectrum is desirable in many aspects. From the viewpoint of theory, this model can be used to study some useful statistics of the aberrated beam, such as beam wandering and spreading. In particular, the universal form of spectrum may lead to a universal form of the optical transfer function. From the viewpoint of simulation, this model can generate random implementation of 2D OPD by using the basic flow parameters. Combining this model and the Kolmogorov model together, the integrated simulation of airborne laser system or optical imaging system is available.

Another contribution of this work is in the application of correlation function in analyzing the statistics of OPD. This tool is almost versatile enough for the examination of random function, but its applicability is often negligible. The correlation function can be discussed reasonably only for stationary random function. For a stationary function, the Fourier transform of its correlation function must be nonnegative, and the converse is also true.[21] For the SPTBL concerned here and studied by Gordeyev *et al.*,[11] the negative part of the power spectrum of OPD indicates the non-stationary characteristic of the aberrated wavefront caused by the flows. In the analysis of velocity of the TBL, the correlation coefficients similar to the ones in Fig. 2 appear frequently,[19,26] especially for the spanwise component. This phenomenon may also imply the non-stationary velocity distribution, and one should be cautious about using this tool.

References

[1] Gilbert K G and Otten L J 1982 *Aero-Optical Phenomena* (New York: AIAA)
[2] Sutton G W 1985 *AIAA J.* **23** 1525
[3] Jumper E J and Fitzgerald E J 2001 *Prog. Aerospace. Sci.* **37** 299
[4] Wang W, Mani A and Gordeyev S 2012 *Ann. Rev. Fluid. Mech.* **44** 299
[5] Gordeyev S, Jumper E J, Ng T T and Cain A B 2003 *AIAA Paper* 2003–3606
[6] Malley M, Sutton G W and Kincheloe N 1992 *Appl. Opt.* **31** 4440

[7] Wittich D, Gordeyev S and Jumper E 2007 *AIAA Paper* 2007-4009
[8] Smith A E, Gordeyev S and Jumper E 2012 *Proc. SPIE* **8395** 83950C
[9] Wang K and Wang M 2012 *J. Fluid Mech.* **696** 122
[10] Wyckham C M and Smits A J 2007 *AIAA Paper* 2006-3067
[11] Gordeyev S, Jumper E and Hayden T E 2012 *AIAA J.* **50** 682
[12] Zhao Y X, Yi S H, Tian L F and Cheng Z Y 2009 *Sci. China Ser. E* **52** 3640
[13] He L, Yi S H, Zhao Y X, Tian L F and Chen Z 2011 *Sci. China Ser. G* **54** 1702
[14] He L, Yi S H, Zhao Y X, Tian L F and Chen Z 2011 *Chin. Sci. Bull.* **56** 489
[15] Gao Q, Yi S H, Jiang Z F, He L and Zhao Y X 2012 *Opt. Express* **20** 16494
[16] Tian L F, Yi S H, Zhao Y X, He L and Cheng Z Y 2009 *Sci. China Ser. G* **52** 1357
[17] Ye Q X and Shen Y H (ed.) 2006 *Practical Handbook of Mathematics* (Beijing, Science Press)
[18] Ganapathisubramani B, Clemens N T and Dolling D S 2006 *J. Fluid Mech.* **556** 271
[19] Hutchins N and Marusic I 2007 *J. Fluid Mech.* **579** 1
[20] Ringuette M J, Wu M and Martin M P 2008 *J. Fluid Mech.* **594** 59
[21] Tatarski V I 1961 *Wave Propagation in a Turbulent Medium* (New York: McGraw-Hill) pp. 9–43
[22] Cliff S F 1978 *Laser Beam Propagation in the Atmosphere*, Strohbehn J W (ed.) (Berlin: Springer-Verlag) pp. 3–26
[23] Lane R G, Glindemann A and Dainty J C 1992 *Waves Rand. Media* **2** 209
[24] Frehlich R 2000 *Appl. Opt.* **39** 393
[25] Smits A and Dussauge J 2006 *Turbulent Shear Layers in Supersonic Flow* (New York: Springer)
[26] Ganapathisubramani B, Hutchins N, Hambleton W T, Longmire E K and Marusic I 2005 *J. Fluid Mech.* **524** 57